1999

Deoxyephedrine -- mandelic acid diastereomers

Edward J. Valente
University of Portland, valentee@up.edu

M. E. Harris

K. Goubitz

H. Schenk

Deoxyephedrine – mandelic acid diastereomers[1]

E. J. Valente*,[I], M. E. Harris[I], K. Goubitz[II] and H. Schenk[II]

[I] Mississippi College, Department of Chemistry, Clinton, MS 39058-4036, USA
[II] Universiteit van Amsterdam, Amsterdam Institute of Molecular Studies, Laboratorium voor Kristallografie, Nieuwe Achtergracht 166, 1018 NV Amsterdam, The Netherlands

Received June 3, 1998; accepted January 19, 1999

Abstract. Resolution of mandelic acid with (−)(*R*)-deoxyephedrine in 95% ethanol produces essentially non-discriminating unsolvated binary mandelate salts. (*R*)-deoxyephedrinium (*R*)-mandelate (**I**) is orthorhombic, $P2_12_12_1$, $a = 8.076(2)$ Å, $b = 8.926(3)$ Å, $c = 23.242(15)$ Å, $V = 1675.3(14)$ Å^3, $Z = 4$. (*R*)-deoxyephedrinium (*S*)-mandelate (**II**) is monoclinic, $P2_1$, $a = 16.061(14)$ Å, $b = 8.902(8)$ Å, $c = 19.585(20)$ Å, $\beta = 111.76(8)°$, $V = 2600(4)$ Å^3, $Z = 6$ with three ion-pairs comprising the asymmetric unit. The principle interionic interactions are ribbon-like chains of salt-bridge hydrogen bonds which associate protonated secondary ammonium ions with carboxylates in **I** and **II** along crystallographic screw axes with a six-atom repeating unit $H{-}N^+{-}H\cdots O{-}C^-{-}O$ [$C_2^2(6)$]. The (*R*)-mandelate additionally shows intraion hydrogen bonding and the (*S*)-mandelate shows interanion hydrogen bonding. Solubilities (in 95% ethanol), fusion points and heats of fusion indicate essentially no diastereometric discrimination. From acetone, the (*S*)-mandelate salt forms a efflorescent hemiacetone solvated binary phase (**III**), triclinic, $P1$, $a = 10.869(9)$ Å, $b = 10.838(13)$ Å, $c = 17.138(18)$ Å, $\alpha = 90.32(9)°$, $\beta = 91.34(8)°$, $\gamma = 108.20(8)°$, $V = 1917(4)$ Å^3, $Z = 4$. Ions form hydrogen bonded chains similar to those in **II**; acetones are unassociated. In **I**, columns form with the polar hydrogen bonded chains at the core and nonpolar aryl rings radiating and interdigitating adjacent columns. Packing in **II** and **III** produces bilayers of alternating polar and nonpolar regions, with acetones of **III** in the nonpolar regions.

Introduction

Organic diastereometric salts form a practical recognition system where extant physical property disparities can be exploited to partially separate enantiomeric components (Jacques, Collet, Wilen, 1981). In a typical system, a racemic organic amine and a chiral organic acid (or *vice versa*) are combined in equimolar ratios, and the diastereomers are separated on the basis of differential solubility in some solvent. Considerable solubility differences can be occasionally achieved such as in the case of the diastereomeric ephedrinium mandelates in water (Jaworski, Hartung, 1943). It is tempting to speculate that clearly identifiable structural characteristics of and differences between diastereomeric salt structures rationally underlay property disparities such as solubility, as well as heats and fusion temperatures. Nevertheless, rational design of diastereomeric resolving systems follows more a pragmatic line based loosely on chemical criteria. Prediction of resolving system success, employing methods such as principle component analysis of the physical parameters for amine resolving agents, is at present fairly unreflective of the more than the broad outlines of binary salt formation, such as the general differences between structurally rigid alkaloid and structurally flexible arylalkylamine bases (Bruggink, 1997).

In previous contributions in this series, detailed studies of the structures and a few relevant physical properties of the ephedrine and pseudoephedrine (halo)mandelates have been described (Valente, Miller, Zubkowski, Eggleston, Shui, 1995; Valente, Moore, Knight-Williams, 1998). The chief interion attractions are the salt-link type hydrogen bonds between bidirectional protonated secondary ammonium and carboxylate groups. These are augmented by interactions involving the hydroxy groups on both the amine and acid components of the diastereomeric salts. Thus, these studies have focused on systems with interacting bidirectional hydrogen bond forming groups with a tendency (but not an unfailing proclivity) toward formation of hydrogen bonded chains. The number of hydrogen bonding donors and acceptors in ephedrine and pseudoephedrine salt-forming moieties are approximately equal, and only rarely do capable groups fail to engage in hydrogen bonding. In fact, the formation of salt-link hydrogen bonds necessarily associates the best donors and acceptors in general agreement with Etter's (1991) rules.

In the present contribution, we examine the resolution of mandelic acid with deoxyephedrine in 95% ethanol. Since deoxyephedrine lacks the ancillary benzylic hydroxy group of the resolving bases ephedrine and pseudoephedrine, this system may serve to probe the effects of removal of a weaker component of hydrogen bonding abil-

[1] Discrimination in resolving systems, part 4. Previous article in the series: Discrimination in resolving systems. III: Pseudoephedrine-mandelic acid. Chirality **10** (1998) 325–337.

* Correspondence author (e-mail: valente@mc.edu)

ity on the properties (solubility, fusion temperatures, heats of fusion), discriminating differences and structural features of the phases formed. A comparison with corresponding features of the ephedrine and pseudoephedrine salts can then be formed.

Experimental

(−)(*R*)-Deoxyephedrine ([α]$_D$ −17.9°, c1.0, 0.1 M HCl) was obtained from Sigma Chemical Co. and (+)(*S*)-, (−)(*R*)- and (±)-mandelic acid were obtained from Aldrich Chemical Co. in their highest available purities. Water-azeotrope ethanol (95%) was obtained from Quantum Chemical Corporation, USI Division; acetone from Fisher Scientific Co. Differential scanning calorimetry (DSC) was performed on a Shimadzu DSC-50 under nitrogen at a heating rate of 10 K/min; the instrument was calibrated against 99.9999% indium and tin. Single crystal diffractometry was carried out on Siemens R3/mV automated diffractometer with graphite monochromatized MoK_α radiation ($\lambda = 0.71073$ Å).

Resolving system: (−)(*R*)-deoxyephedrine and (±)-mandelic acid

Equimolar quantities of the base and acid were combined in 95% ethanol and dissolved with warming to 323 K using 800 mg solute per mL solvent. On cooling to 263 K and evaporating solvent, crystallization of both diastereomeric salts occurs slowly, simultaneously and only after most of the solvent has left. DSC of representative samples taken from the crystallizing solution show two distinct melting phases at 370 K and 382 K. Where (+)(*S*)-mandelic acid or (−)(*R*)-mandelic acid and (−)-deoxyephedrine were combined in equimolar proportions either neat or in 95% ethanol, exothermic reactions ensued from which colorless salts were obtained. The resulting solid phases were recrystallized from 95% ethanol. An analytical sample of (−)(*R*)-deoxyephedrinium (+)(*R*)-mandelate (**I**) was obtained as colorless elongated prisms from 95% ethanol. An analytical sample of (−)(*R*)-deoxyephedrinium (−)(*S*)-mandelate (**II**) was obtained as colorless thin columnar prisms from 95% ethanol, benzene or ethyl ethanoate; the phase from each recrystallization is the same by DSC. Upon recrystallization of **II** from acetone, large colorless prismatic plates (**III**) form which contain a half equivalent of acetone of crystallization. DSC analysis shows loss of acetone: 329 K (onset), 341.8 (peak), desolvated material fuses at 364.4 K (peak), with partial recrystallization to phase **II**, mp 370.4 K (peak). Solubility and differential scanning calorimetric data on **I** and **II** are given in Table 1.

Table 1. Solubility and differential scanning calorimetric data for (−)(*R*)-deoxyephedrine mandelates from 95% ethanol.[a]

Phase	Mandelate configuration	Solubility g/100 mL, 95% ethanol	Heat of fusion kJ/mol	Fusion temperature K
	R	31.2(10)[b]	−31.0(13)	382.8(2)
I	*S*	32.4(32)[c]	−29.8(33)	371.5(2)

[a] Estimated standard deviation in parentheses.
[b] At 292.3 K.
[c] At 291.6 K.

Crystallography

A summary of the crystallographic data and aspects of the crystallographic experiment are given in Table 2. Crystals of **III** lost solvent on exposure to air over a few days; the crystallographic specimen was wedged in the top of a 0.5 mm glass capillary, placed in contact with a small portion of its saturated acetone solution, and sealed with beeswax. Programs used were SHELXL-90 (**I**, **II**) and CRUNCH (**III**) for structure discovery and SHELXL-97 for fullmatrix least-squares refinement (Sheldrick, 1993; 1997; de Gelder, de Graaff, Schenk, 1990; 1993). An approximate monoclinic cell for **III** is not supported by the lack of symmetry of the cell contents. Scattering factors were taken from the *International Tables for X-Ray Crystallography* (1992). Models included the atomic positions and anisotropic displacement parameters for all non-H atoms. Models were refined against all unique data. Absolute configuration of mandelates were assigned based on the known configuration of (−)(*R*)-deoxyephedrine. In **II** and **III**, no evidence for disorder could be found in phenyl rings for which librations appreciate considerably toward their distal ends. Acetones in **III** also have large librations, and an approximate trigonal disorder of atoms around the central carbon is possible. The model is insensitive to such a treatment, so the oxygen was assigned to the atom terminating the shortest trigonal distance found in each solvate molecule. Coordinates and equivalent isotropic vibrational values are given in Tables 3–5 for phases **I**, **II**, and **III**, respectively.[2] Most H-atom positions were calculated and allowed to contribute to the model with isotropic vibrational factors 20% larger than the equivalent isotropic vibrational factors of the attached atom (except H's in acetones, 50% larger). Special attention was given to location of the H-atoms on the hydroxy donor groups of **I** and **II**. Because of the intrinsic insensitivity of the x-ray experiment and the limits of resolution of the determinations, it is difficult to accurately locate hydroxy H-atoms. In the least-squares refinements, positions of the hydroxy H's were assigned based on a search of difference maps for a peak in density around the oxygens; calculated positions were adjusted in least-squares with refinement of the torsion angles about the C–O bond. In all cases, the torsion angle refined without problem and inspection of the difference maps showed no ambiguity about the assigned H-atom locations. The OH

[2] Supplementary Material: Crystallographic data (excluding structure factors) for the structures reported in this paper have been deposited with the Cambridge Crystallographic Data Centre as supplementary publication no. 118705, 118706, 118707. Copies of available material can be obtained, free of charge, on application to CCDC, 12 Union Road, Cambridge CB2 1EZ, UK, (fax: +44-(0)1223-336033 or e-mail: deposit@chemcrys.cam.ac.uk). The list of F_o/F_c-data is available from the author up to one year after the publication has appeared.

Table 2. Crystallographic data for (−)(*R*)-deoxyephedrine salts of (*R*)-mandelic (**I**), (*S*)-mandelic acid (**II**) from 95% ethanol, and (*S*)-mandelic acid (**III**) from acetone.

	I	**II**	**III**
Formula	$(C_{10}H_{16}N)^+ (C_8H_7O_3)^-$	$(C_{10}H_{16}N)^+ (C_8H_7O_3)^-$	$(C_{10}H_{16}N)^+ (C_8H_7O_3)^- \cdot {}^1/_2\, C_3H_6O$
Formula weight	301.37	301.37	$301.37 + {}^1/_2$ (58.08)
Specimen size, (mm)	0.3 × 0.3 × 0.7	0.04 × 0.1 × 1.0	0.2 × 0.4 × 0.6
Temperature, (K)	292(2)	292(2)	292(2)
Crystal system	orthorhombic	monoclinic	triclinic
Space group	$P2_12_12_1$ (#19)	$P2_1$ (#4)	$P1$ (#1)
a, (Å)	8.076(2)	16.061(14)	10.869(9)
b, (Å)	8.926(3)	8.902(8)	10.838(13)
c, (Å)	23.242(15)	19.585(20)	17.138(18)
α, (°)	90	90	90.32(9)
β, (°)	90	111.76(8)	91.34(8)
γ, (°)	90	90	108.20(8)
Volume, (Å^3)	1675.3(14)	2600(4)	1917(4)
Refl. detng. lattice	50	50	38
Z, ion-pairs/cell	4	6	4
D_{calc}, (Mg/m^3)	1.195	1.155	1.145
μ, (mm^{-1})	0.08	0.08	0.08
θ_{max}, (°)	32.5	25.0	21.0
Scan type, width (°)	ω, 1.8	ω, 1.3	ω, 2.0
Quadrants measured	1	1	2.3
Decay, (%)	−1(1)	−1(1)	−10(3)
Intensities (all; $> 2\sigma_I$)	6080; 2045	4902; 1800	5482; 2500
R_{int} (on F)	0.06	0.11	0.13
Variables	203	596	863
R (all; $I > 2\sigma_I$)	0.119; 0.064	0.144; 0.070	0.128; 0.090
wR (all)	0.159	0.171	0.221
S ($I > 2\sigma_I$)	0.956	1.033	0.953
$\varrho_{residual}^{max;min}$ (e$^-$/Å^3)	0.20; −0.23	0.27; −0.33	0.30; −0.59
weight factor[a], P	0.092	0.091	0.135

a: Weights = $1/\{\sigma_{F_o}{}^2 + P\,[\max(F_o{}^2, 0) + 2F_c{}^2/3]^2\}$

Table 3. Atomic coordinates (×10^4) and equivalent isotropic displacement parameters (Å^2 × 10^3) for (−)(*R*)-deoxyephedrinium (*R*)-mandelate (**I**). U_{eq} is defined as one third of the trace of the orthogonalized U^{ij} tensor.

Atom	x	y	z	U_{eq}
O1	691(3)	3995(2)	3768(1)	68(1)
O2	736(2)	6502(2)	2570(1)	53(1)
O3	−86(2)	6737(2)	3478(1)	61(1)
N	297(2)	4794(2)	1599(1)	45(1)
C1	4419(3)	5105(3)	811(1)	47(1)
C2	5064(3)	6546(3)	801(1)	52(1)
C3	6211(4)	6975(3)	393(1)	63(1)
C4	6705(4)	5992(4)	−22(1)	68(1)
C5	6094(4)	4552(4)	−13(1)	72(1)
C6	4966(3)	4118(3)	394(1)	61(1)
C7	3142(3)	4670(3)	1252(1)	51(1)
C8	1416(3)	5241(3)	1111(1)	45(1)
C9	755(4)	4614(3)	552(1)	66(1)
C10	−1473(3)	5222(3)	1523(1)	59(1)
C11	3046(3)	4352(2)	3143(1)	41(1)
C12	3751(3)	3369(3)	2755(1)	49(1)
C13	5447(3)	3259(3)	2696(1)	64(1)
C14	6459(3)	4129(4)	3032(1)	71(1)
C15	5794(3)	5097(3)	3416(1)	67(1)
C16	4090(3)	5217(3)	3474(1)	57(1)
C17	1194(3)	4447(2)	3212(1)	43(1)
C18	568(3)	6092(2)	3073(1)	41(1)

and NH distances were assigned lengths during the refinements of 0.82 Å and 0.90 Å, respectively, reflecting the usual bias in the x-ray determination. In subsequent calculations for hydrogen bonding, the positions were reassigned such that the OH and NH distances became 0.96 Å and 1.00 Å, the former along the vector determined from the torsion angle refinements. Since the geometric limits of the components of three-center hydrogen bonds are arguable, they were considered present if the angle at the donor atom (O, N) exceeded 90° and the sum of the angles of the contact atoms at H is 340°–360° (Jeffrey, Saenger; 1991). Hydrogen bonded arrays are described with the aid of the terminology of Etter, McDonald, Bernstein (1989).

Solubility

In tared vials, 15–30 mg samples of the recrystallized salts **I** and **II** were weighed and 30–50 µL of 95% ethanol was introduced with calibrated micropipettes. On sealing, the samples were agitated for 2 h at 291 K–292 K until saturated solutions were produced. The solution was removed by micropipette and transferred to a second tared vial; the pipette was washed with 95% ethanol and the washes added to the second vial. Solvent in both vials was then carefully removed under a gentle stream of air. Solubilities were determined in duplicate. Errors were deduced from the recoveries of the salts; range 100–110%; mean 105%, esd 10%. Solubilities and DSC results are presented in Table 1.

Table 4. Atomic coordinates ($\times 10^4$) and equivalent isotropic displacement parameters ($Å^2 \times 10^3$) for (−)(*R*)-deoxyephedrinium (*S*)-mandelate (**II**). U_{eq} is defined as one third of the trace of the orthogonalized U^{ij} tensor.

Atom	*x*	*y*	*z*	U_{eq}	Atom	*x*	*y*	*z*	U_{eq}
O1A	5408(3)	−8571(6)	4382(2)	68(2)	C8B	8078(4)	−2426(8)	9620(4)	47(2)
O2A	4941(3)	−5766(5)	4754(2)	59(1)	C9B	8264(5)	−4098(9)	9837(4)	66(2)
O3A	6352(3)	−5347(6)	5466(3)	62(1)	C10B	9641(4)	−1516(10)	1023(4)	65(2)
N1A	6441(4)	−2597(7)	6113(3)	61(2)	C11B	6736(4)	2490(8)	7698(4)	49(2)
C1A	7999(6)	−1506(10)	5148(6)	77(3)	C12B	6297(4)	2813(10)	6964(4)	67(2)
C2A	7968(7)	−393(13)	4627(5)	97(3)	C13B	5450(5)	2220(12)	6570(5)	87(3)
C3A	8701(10)	7(16)	4472(7)	130(5)	C14B	5056(5)	1288(12)	6923(5)	82(3)
C4A	9514(10)	−620(2)	4873(10)	147(6)	C15B	5487(5)	961(10)	7650(5)	75(3)
C5A	9580(8)	−1712(16)	5408(9)	148(6)	C16B	6330(4)	1522(10)	8026(4)	63(2)
C6A	8829(7)	−2094(11)	5539(7)	116(4)	C17B	7667(4)	3091(8)	8132(4)	51(2)
C7A	7186(5)	−1952(10)	5274(5)	71(2)	C18B	8345(4)	1798(8)	8386(4)	49(2)
C8A	7287(5)	−1974(9)	6072(4)	65(2)	O1C	9952(3)	−749(6)	8730(2)	57(1)
C9A	7493(6)	−422(12)	6443(5)	108(3)	O2C	9091(3)	−3509(6)	8430(3)	62(1)
C10A	6447(5)	−2805(10)	6871(4)	83(3)	O3C	9378(3)	−3715(6)	7418(3)	68(2)
C11A	6491(5)	−7011(10)	4146(4)	62(2)	N1C	9211(3)	−6612(7)	7017(3)	53(2)
C12A	6152(6)	−7603(12)	3440(5)	87(3)	C1C	11713(5)	−7362(12)	7928(5)	78(3)
C13A	6531(7)	−7098(15)	2942(6)	111(4)	C2C	12133(7)	−6670(16)	7540(7)	134(5)
C14A	7201(8)	−6127(15)	3112(6)	107(4)	C3C	13036(8)	−7000(2)	7667(9)	151(6)
C15A	7554(6)	−5550(14)	3811(7)	106(4)	C4C	13468(9)	−7990(2)	8210(9)	155(8)
C16A	7185(5)	−6014(10)	4323(5)	74(3)	C5C	13042(8)	−8700(2)	8583(7)	141(6)
C17A	6091(5)	−7511(8)	4701(4)	57(2)	C6C	12157(6)	−8437(14)	8456(5)	102(4)
C18A	5758(5)	−6051(8)	4993(4)	51(2)	C7C	10753(4)	−6986(11)	7820(4)	77(3)
O1B	7886(3)	4189(5)	7687(3)	63(1)	C8C	10098(5)	−7086(9)	7026(4)	58(2)
O2B	8833(3)	1527(6)	8020(3)	60(1)	C9C	10076(5)	−8629(10)	6698(4)	83(3)
O3B	8362(3)	1091(6)	8925(3)	61(1)	C10C	8513(5)	−6529(9)	6281(4)	68(2)
N1B	8860(3)	−1710(7)	9541(3)	51(2)	C11C	11055(4)	−2380(8)	8600(4)	49(2)
C1B	6439(5)	−2903(10)	8911(4)	63(2)	C12C	11598(6)	−2668(14)	8212(5)	107(4)
C2B	6091(6)	−4235(12)	8518(5)	84(3)	C13C	12454(6)	−3228(16)	8545(7)	139(6)
C3B	5322(6)	−4877(14)	8531(6)	118(4)	C14C	12771(6)	−3568(14)	9279(6)	110(4)
C4B	4937(8)	−4270(2)	8993(9)	148(6)	C15C	12238(5)	−3355(11)	9652(5)	81(3)
C5B	5225(8)	−2980(2)	9364(8)	152(6)	C16C	11387(5)	−2801(9)	9325(4)	63(2)
C6B	6011(6)	−2319(15)	9324(6)	112(4)	C17C	10132(4)	−1755(9)	8246(4)	52(2)
C7B	7291(4)	−2286(9)	8883(4)	58(2)	C18C	9472(5)	−3107(9)	8017(5)	55(2)

Discussion

Binary (−)(*R*)-deoxyephedrinium (−)(*R*)-mandelate (**II**) crystallizes as the very slightly less-soluble of the two unsolvated diastereomeric phases obtained from a mixture of the base with the racemic acid in 95% ethanol. The more-soluble phase **II** contains the (+)(*S*)-mandelate; three ion-pairs (labeled A, B, C) comprise the asymmetric unit. The degree of solubility discrimination is about 3% indicating that substantial co-precipitation can occur on crystallization under conditions approaching equilibrium, a result which describes the observations on the resolving system. The higher fusion temperature of **I** is consistent with its lower solubility and higher heat of fusion compared with **II**, but the differences are essentially insignificant. However, packing efficiency is better for **I** as judged by the volume per ion-pair of 419 $Å^3$ compared with 433 $Å^3$ for **II**. This compares with 412 $Å^3$ for the less-soluble (−)-ephedrinium (*R*)-mandelate and 429 $Å^3$ for the highest melting more-soluble (−)-ephedrinium (*S*)-mandelate phase (Valente et al., 1995) all of which were obtained from 95% ethanol solutions. This is a significant difference, since deoxyephedrinium ion lacks the benzylic hydroxyl group relative to the ephedrinium salts and yet its mandelate salts are each higher in volume. A reduced molecular volume for the deoxy base is more than offset by a change in packing efficiency compared to the corresponding salts with (−)-ephedrine. The ion-pair volumes of **I** and **II** are 10–20 $Å^3$ smaller that those of the pseudoephedrinium mandelates (Valente, Moore, Williams-Knight, 1998). This is consistent with the smaller volume of the deoxy cation. Diastereomeric deoxyephedrinium and pseudoephedrinium mandelates have generally poorer discriminatory properties than the ephedrinium mandelates.

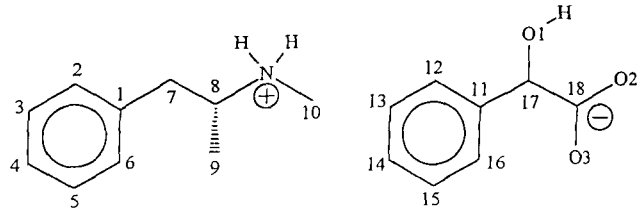

(R)-deoxyephedrinium mandelate

All hydrogen bond donor and acceptor groups are engaged in **I** and **II** (Table 6). A deoxyephedrinium ion can donate two hydrogen bonds but it has no acceptor groups. A mandelate ion has a donor hydroxy group, and the oxygens of its carboxylate groups usually accept three or four hydrogen bonds. The number of donors and acceptors on each ion are mismatched and the presence of inter- and intra-anion hydrogen bonding or inclusion of solvent are plausible structural consequences. Neither salts **I** or **II** ob-

Table 5. Atomic coordinates ($\times 10^4$) and equivalent isotropic displacement parameters ($Å^2 \times 10^3$) for (−)(*R*)-deoxyephedrinium (*S*)-mandelate hemiacetone solvate (**III**). U_{eq} is defined as one third of the trace of the orthogonalized U^{ij} tensor.

Atom	*x*	*y*	*z*	U_{eq}
N1A	3082(8)	9430(9)	6538(5)	66(3)
C1A	2103(12)	7766(14)	8461(8)	85(4)
C2A	1387(18)	8432(17)	8922(10)	122(6)
C3A	1270(3)	8220(3)	9682(11)	174(11)
C4A	1900(3)	7580(3)	10099(11)	195(13)
C5A	2660(3)	6940(2)	9687(14)	164(9)
C6A	2713(16)	7028(17)	8883(10)	112(5)
C7A	2206(12)	7966(12)	7605(6)	72(3)
C8A	3323(11)	9099(13)	7368(7)	69(3)
C9A	4668(12)	8874(15)	7436(8)	92(4)
C10A	4039(12)	10630(13)	6224(7)	81(4)
O1A	7617(7)	10045(8)	6341(4)	73(2)
O2A	9421(8)	9014(9)	5786(5)	75(2)
O3A	10854(9)	10083(9)	6711(5)	82(3)
C11A	8461(11)	9645(12)	7585(6)	56(3)
C12A	7757(11)	8383(13)	7642(8)	72(3)
C13A	7441(14)	7805(17)	8359(11)	99(5)
C14A	7890(2)	8600(3)	9022(11)	125(7)
C15A	8595(18)	9860(2)	8980(8)	105(5)
C16A	8871(13)	10392(15)	8250(7)	82(4)
C17A	8778(10)	10294(12)	6802(6)	60(3)
C18A	9745(11)	9661(13)	6354(8)	66(3)
N1B	7124(9)	8664(9)	4907(5)	66(3)
C1B	8903(14)	9683(15)	3029(8)	91(4)
C2B	9668(19)	9010(2)	2683(10)	142(8)
C3B	9870(3)	9110(3)	1876(15)	192(12)
C4B	9380(3)	9880(3)	1461(13)	199(13)
C5B	8560(3)	10480(3)	1758(13)	184(11)
C6B	8316(17)	10380(2)	2572(11)	134(7)
C7B	8636(13)	9544(13)	3882(7)	80(4)
C8B	7487(12)	8428(11)	4094(6)	64(3)
C9B	7715(14)	7124(14)	4022(8)	91(4)
C10B	5999(13)	7704(13)	5217(7)	83(4)
O1B	6704(8)	14205(8)	5075(5)	76(2)
O2B	7624(8)	12299(8)	5616(5)	76(2)
O3B	6466(9)	10914(9)	4745(5)	81(2)
C11B	7006(12)	13332(11)	3840(6)	58(3)
C12B	6258(15)	12937(14)	3172(8)	90(4)
C13B	6820(2)	13202(18)	2437(8)	112(6)
C14B	8130(2)	13887(18)	2411(10)	111(6)
C15B	8893(18)	14305(17)	3076(10)	110(5)
C16B	8291(14)	14041(13)	3782(7)	76(4)
C17B	6410(11)	13032(11)	4626(6)	62(3)
C18B	6877(12)	12008(12)	5041(7)	61(3)
N1C	8097(8)	4459(9)	6561(5)	63(2)
C1C	9049(15)	4419(15)	8724(7)	89(4)
C2C	10181(16)	4050(2)	8864(9)	123(6)
C3C	10432(18)	3566(19)	9561(11)	128(6)
C4C	9630(2)	3430(2)	10170(12)	154(8)
C5C	8500(3)	3710(3)	10025(13)	195(12)
C6C	8240(2)	4220(3)	9337(9)	162(10)
C7C	8766(15)	4950(14)	7956(7)	87(4)
C8C	8354(12)	3939(12)	7333(6)	66(3)
C9C	7150(14)	2832(14)	7501(7)	86(4)
C10C	9228(12)	5584(14)	6270(8)	97(4)
O1C	2619(8)	4881(9)	6558(5)	76(2)
O2C	4558(8)	4160(9)	5896(5)	76(2)
O3C	5997(8)	5365(8)	6775(5)	77(2)
C11C	3515(12)	4080(13)	7652(6)	60(3)
C12C	4256(13)	4416(15)	8343(9)	88(4)
C13C	4033(16)	3490(2)	8943(8)	102(5)
C14C	3125(17)	2365(16)	8842(9)	94(4)
C15C	2402(14)	1999(16)	8180(8)	88(4)
C16C	2632(13)	2919(14)	7607(7)	72(3)
C17C	3781(11)	5059(12)	6993(6)	67(3)
C18C	4893(11)	4835(11)	6485(7)	60(3)
N1D	2279(7)	3554(7)	4988(4)	68(3)
C1D	2133(7)	2844(7)	2796(4)	97(5)
C2D	2578(7)	1810(7)	2611(4)	118(5)
C3D	3030(2)	1780(3)	1850(14)	188(12)
C4D	3020(3)	2600(3)	1320(11)	170(11)
C5D	2580(3)	3680(3)	1483(13)	167(9)
C6D	2133(17)	3755(19)	2239(9)	117(5)
C7D	1647(13)	2994(15)	3617(8)	90(4)
C8D	2739(12)	3358(13)	4199(6)	71(3)
C9D	3827(13)	4592(14)	3995(8)	88(4)
C10D	1266(14)	2468(14)	5281(8)	95(4)
O1D	1687(8)	8989(8)	5045(4)	74(2)
O2D	1408(8)	5655(10)	4832(5)	76(2)
O3D	2585(8)	7086(8)	5702(5)	72(2)
C11D	2447(13)	8139(12)	3933(7)	62(3)
C12D	2109(17)	7412(17)	3247(10)	107(5)
C13D	2950(2)	7656(18)	2614(9)	117(6)
C14D	4110(2)	8595(19)	2676(10)	109(5)
C15D	4406(17)	9290(17)	3348(11)	109(5)
C16D	3597(13)	9082(14)	3969(8)	77(4)
C17D	1551(11)	7837(11)	4617(7)	62(3)
C18D	1896(12)	6785(13)	5103(7)	63(3)
Acetone solvate				
O1S	5472(19)	1920(2)	10444(12)	225(10)
C2S	5430(3)	690(3)	9363(14)	195(12)
C3S	5440(2)	790(3)	10206(14)	150(8)
C4S	5420(4)	−260(5)	10620(2)	370(4)
O5S	5140(4)	6720(5)	930(2)	510(4)
C6S	5970(3)	6300(3)	2018(17)	232(15)
C7S	5990(4)	6260(3)	1160(2)	250(2)
C8S	6890(6)	5960(5)	780(2)	430(5)

Table 6. Hydrogen bonding (H···O) distances (Å) and angles (at H, °) for (−)-deoxyephedrinium mandelates (**I**) and (**II**) arranged by donor-acceptor pairs.[a]

Anion Phase Donor-Acceptor	(*R*)-mandelate (**I**)	(*S*)-mandelate (**II**)		
		A	B	C
Inter-counterion hydrogen bonding				
$^+NH \cdot O_2C^-$	1.78, 161	**1.75, 168**	**1.76, 178**	**1.71, 163**
$^+NH \cdot O_2C^-$ chain	1.80, 158	**1.78, 173**	**1.86, 166**	**1.82, 169**
$^+NH \cdot OH$		*2.64, 95*	*2.68, 92*	*2.67, 98*
		2.52, 102	*2.43, 108*	*2.57, 104*
Intercation and interanion hydrogen bonding				
$OH \cdot O_2C^-$		1.84, 164	1.88, 166	**1.77, 175**
				2.59, 119
Intraion hydrogen bonding				
$OH \cdot O_2C^-$	2.11, 112			

a: Two-center and three-center H-bonds; for the latter, strong component in **boldface** given above its corresponding weaker arm in *italics*; sum of angles at H: 340–360°; N–H distances normalized to 1.00 Å; O–H to 0.96 Å.

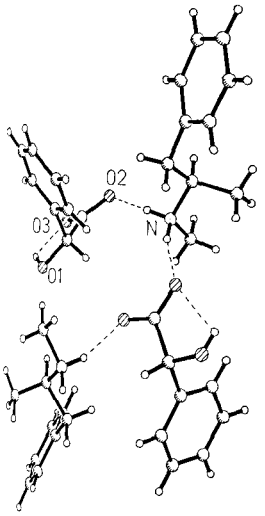

Fig. 1. Plot of the structure of **I** showing two ion-pairs and the chain hydrogen bonding.

tained from the resolving system solvent (95% ethanol) contain solvent of crystallization; salt **III** contains unassociated acetones. The strongest hydrogen bonds are those in helical chains linking ion-pairs in **I** and **II** through their secondary ammonium and mandelate carboxylate groups with a six-atom repeat $H-N^{+}-H\cdots O-C^{-}-O$, $C_2^2(6)$. In I, this involves a chain through screw-related ions along *b* (8.93 Å) with two ion-pairs in the crystallographic repeat. Along *b*, nitrogens in the hydrogen bonded chain are spaced 6.14 Å distant and are well isolated from neighboring chains. Mandelate ions additionally show intraionic hydrogen bonds with pattern $R_1^1(5)$, and the carboxylate carbons (C18) are separated by 5.28 Å. Hydrogen bonding liasons occur on the interior of columns with phenyl rings from each ion type radiating and weakly interlocking with those of adjacent columns. In **II**, there are three similar hydrogen bonded strands: one in which the "A" ion-pair forms a chain alternating with its screw-relative ions (Fig. 2), and two chains in which the "B" ion-pair forms a chain alternating with the screw-relative of

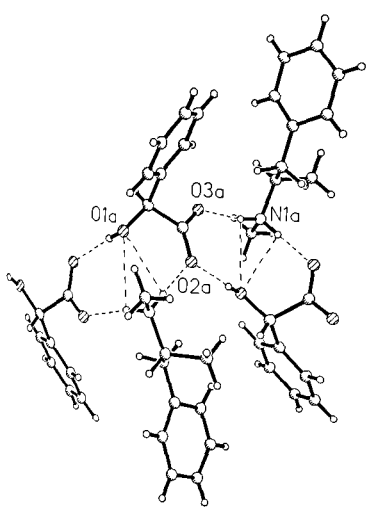

Fig. 2. Plot of a portion of the structure of **II** showing the chain hydrogen bonding between the "A" molecules.

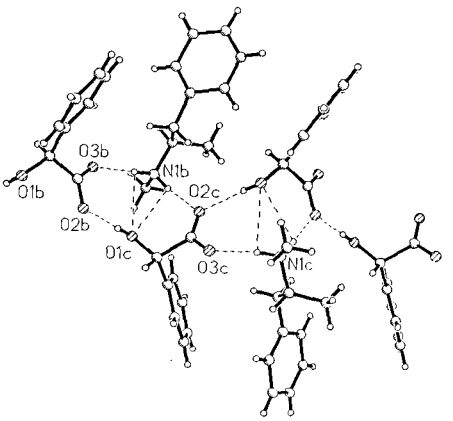

Fig. 3. Plot of a portion of the structure of **II** showing the chain hydrogen bonding between the "B" and "C" molecules.

the "C" ion-pair (Fig. 3) and *vice versa*. Each chain extends along *b* (8.90 Å) with two ion-pairs in the crystallographic repeat. Nitrogens in the "A" chain are spaced 6.73 Å distant along *b*; nitrogens in the "BC" chains are spaced 6.77 Å and 6.87 Å distant; they are closer to two N's in neighboring chains within the polar region. Carboxylate carbons are closer than are the N's to the screw axis and are separated along chains by 4.88 Å, 5.03 Å, and 5.08 Å. Both N–H's of each cation also face and weakly donate in a bifurcated hydrogen bond to a neighboring mandelate hydroxy oxygen forming rings with $R_2^1(4)$ pattern. Interanion hydrogen bonds link hydroxy and carboxylates within a chain forming embedded rings with pattern $R_3^3(11)$. Consequently, an alternate hydrogen bonded path with a six-atom repeat occurs through mandelates $O-C(O)-C-O-H\cdots O-C(O)^{-}$ with pattern $C_1^1(6)$; it crosses the salt-link chain and these are further cross-linked by bifurcated $^{+}NH_2\cdots OH$, forming $R_2^1(4)$ rings within the chains. Bilayers of ion-pairs are found with layers forming perpendicular to the *b* axis and along the *ac* diagonal with a thickness of about 14.8 Å. Hydrogen bonded chains in **I** or **II** are not crosslinked with other chains through the mandelate ions; such a feature lends considerable stability to some less-soluble ephedrinium salts (Valente et al., 1995).

Non-polar group phenyl ring packing (columns in **I** and layers in **II**) shows an additional comparative difference of significance for crystal stability. Examination of the U_{eq}'s for the distal three carbons of both deoxyephedrinium (C3, 4, 5) and mandelate (C13, 14, 15) phenyl rings shows that at 292 K, the motion of these atoms implied by the U's is significantly greater for **II** (143, 110 Å^2) than for **I** (68, 67 Å^2), a rough guide to the packing restrictions imposed on these portions of the ions. Since the fusion points for the diastereomers differ by only 11 K and average about 80 K above the x-ray experimental temperature, this difference indicates less vibrational restriction in **II**, which is consistent with its decreased packing efficiency and lower fusion point.

Four ion-pairs (labeled A, B, C, D) and two acetone molecules comprise the asymmetric unit in the triclinic acetone-solvated structure **III**. From an inspection of the donor and acceptor atom contacts in **III** (Fig. 4), it seems likely that its interion hydrogen bonded contacts are as in

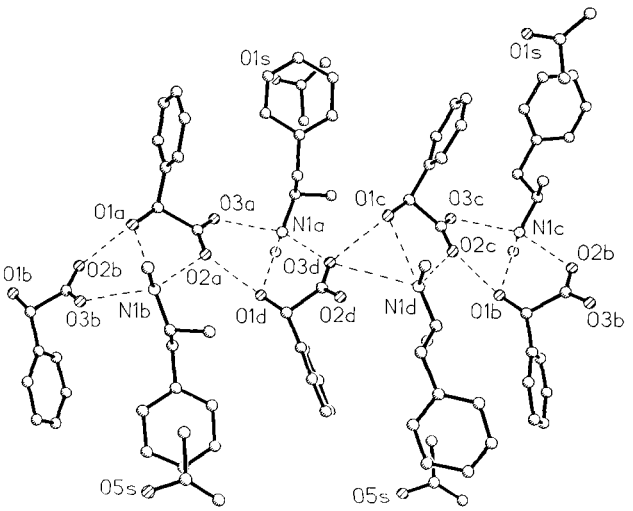

Fig. 4. Plot of the structure of **III** showing the chain hydrogen bonding contacts.

phase **II**. The chains involve the shorter, stronger components of the $^{+}N-H\cdots O^{-}$ hydrogen bonds and extend zig-zag fashion across the *a*–*b* face. The four inequivalent ion-pairs are related by translation with a crystallographic repeat of 17.58 Å. Nitrogens in the hydrogen bonded chain in **III** are farther apart than in **I** but about the same as in **II**, the inter-nitrogen distances being 6.80 Å (A–B), 6.64 Å (B–C), 6.60 Å (C–D), and 6.68 Å (D–A). Carboxylate carbons are also about as separated along the chains as in **II** with distances of 4.94 Å, 4.95 Å, 4.97 Å and 5.09 Å. Shorter N···N distances can be found between N's on neighboring chains within the polar region. Bilayer packing occurs in **III** with 17.1 Å layers forming perpendicular to the *c* axis. Acetone solvate molecules loosely pack between phenyl rings in the non-polar portion of the bilayer. As in **II**, ion-packing efficiency in **III** is also poorer than in **I**, and the mean U_{eq}'s of the distal three phenyl ring carbons are 176 and 107 Å^2 for the cation and anion, respectively. Acetones in this same region have even higher librations with mean U_{eq}'s of 235 and 356 Å^2 for the four non-H atoms. The location of the acetones and librations are consistent with the efflorescent behavior of the phase.

Deoxyephedrinium ions in **I**, **II**, and **III** A, B have the fully-extended conformation with the two characteristic torsions near 180° (Table 7); **III** C and D have the *anti*, *gauche* conformation. In the mandelate ions, the hydroxy oxygen is roughly aligned (±30°) with one of the carboxylate oxygens, a conformation which is commonly found in mandelates and mandelic acids (Acs, Novotny-Bregger, Simon, Argay; 1992; Larsen, deDiego, 1993). Such a conformation is supportive of intraionic hydrogen bonding, though identified only in salt phase **I**.

Both of the unsolvated diastereomeric salts **I** and **II** have salt-bridge $C_2^2(6)$ hydrogen bonded chains as the dominant interionic cohesive interaction. Polar and nonpolar groups are both found with typical associations. Hydrogen bonded polar groups concentrate along well-defined directions. In **I** and **II**, the hydrogen bonding is along crystallographic axes. In the (*S*)-mandelates (**II**, **III**), a concentrated ribbon of hydrogen bonds links ions without intraionic mandelate interactions. In **II**, where cations are in the fully extended conformation, the chiral methyl of the cation points above and along the ribbon direction, and the chiral phenyl of the anion is oriented to the opposite side of the hydrogen bonded ribbon (Fig. 2, 3). In **III**, the same staggering of methyls and phenyls along the hydrogen bonded ribbon occurs for half of the ion-pairs (A and B) on both sides of the ribbon. Without a change in the repeat pattern, the ribbon then accomodates the next two ion-pairs (C and D) with cations in the *anti*, *gauche* conformation where the chiral methyl of the base (cation) points normal to the ribbon direction, the chiral benzyl group of the base (cation) and the chiral phenyl of the acid (anion) are displayed on the opposite sides of the hydrogen bonded ribbon.

In summary, (−)-deoxyephedrine forms very weakly discriminating diastereomeric phases with mandelic acid compared with (−)-ephedrine (Valente et al., 1992). Loss of the the benzylic hydroxy on the base (cation) precludes interionic hydroxy-carboxylate or hydroxy-hydroxy hydrogen bonding which was evident in the ephedrine mandelates. A somewhat comparable structural change in a resolving system was studied in the diastereomers of 1-phenyl-1-ethanamine and mandelic acid or 2-phenylpropanoic acid (Brianso, 1981) for which solubility differences were affected. Intraionic and three-center hydrogen bonding are more important in the deoxyephedrine mandelates than in ephedrine salts which have more equal numbers of hydrogen bond donors and acceptors. In terms of discrimination, the dominant structural feature in all three deoxyephedrine salts is the chain hydrogen bonding which links the best donors and acceptors. With this selection, accep-

Table 7. Torsion angles descriptive of the conformations of the ions in (−)(*R*)-deoxyephedrinium mandelates, **I**, **II** and **III** (acetone solvate)

Ion	Torsion angles[a], degrees				
	(*R*)-deoxyephedrinium			mandelate	
	C2–C1–C7–C8	C1–C7–C8–N^{+}	C7–C8–N^{+}–C10	C12–C11–C17–C18	HO1–C17–C18–O^{-}
I	78	−177	178	−120	8
II, A	−130	−174	176	−124	−19
II, B	−111	−177	170	−115	−24
II, C	53	−177	176	93	−25
III, A	88	−163	174	−67	−6
III, B	−87	−163	178	110	−13
III, C	74	−179	55	87	−23
III, D	70	178	56	88	−21

a: Estimated standard deviations less than about 2°.

tors of hydrogen bonds from mandelate hydroxy are limited to intra- or interionic carboxylate oxygen or other mandelate hydroxy groups. Intraionic hydrogen bonds occur within mandelates in **I**. Mandelate hydroxy H's in **II** and **III** form interanion hydrogen bonds with neighboring mandelate carboxylates. This description is essentially identical to that comparing the diastereomeric salts of (*R*)-*t*-butyl-3-methylimidazolidin-4-one (BMI) with mandelic acid (Acs, Novotny-Bregger, Simon, Argay; 1992). However, the BMI mandelates were strongly discriminatory in melting temperatures and solubility (though the solvent employed for preparation of the crystallographic specimens was not the same as that used in the resolving mixture). It is noteworthy that in **II**, the addition of interanion interactions is accompanied by an increase in volume of an ion-pair of 15 $Å^3$ (3.5%) compared with **I**. As anions are associated with more hydrogen bonds along the hydrogen bonded chains, the cations are further apart as judged by the distances between N's. Any stability provided by an increase in hydrogen bonded contacts between ions is therefore offset in the deoxyephedrinium mandelates by decreased overall packing efficiency. Since the diastereomers have similar thermal properties and solubilities in 95% ethanol, these disparate structural features underlie their relatively small discriminating property differences.

Acknowledgments. We thank Dr. Jeffrey D. Zubkowski for access to diffraction equipment and the Office of Naval Research for support of this work. Additionally, we acknowledge the support of the National Science Foundation (grant DUE9250669) for support of thermometric equipment.

References

Acs, M.; Novotny-Bregger, E.; Simon, K.; Argay, G.: Structural aspects of optical resolutions. Optical resolution of (*R,S*)-mandelic acid. DSC and x-ray studies of the diastereoisomeric salts. J. Chem. Soc. Perkin Trans. **2** (1992) 2011–2017.

Brianso, P. M.-C.: Sels diastéréomères de phényl-1 ethylamine et d'acides phenylacétiqués α substitutes *p* et *n*. Séparation ou syncristallisation; une explication crystallographique. Acta Crystallogr. B**37** (1981) 618–620.

Bruggink, A.: Rational Design in Resolutions, in Ch. 5 of Chirality in Industry, II, (Collins, A. N., Sheldrake, G. N. and Crosby, J., editors), John Wiley, New York, 1997.

Etter, M.; Hydrogen bonds as design elements in organic chemistry. J. Phys. Chem. **95** (1991) 4601–4610.

Etter, M.; MacDonald, J. C.; Bernstein, J.: Graph-set analysis of hydrogen bond patterns. Acta Crystallogr. B**46** (1989) 256–262.

de Gelder, R.; de Graaff, R. A. G.; Schenk, H.: On the construction of Karle-Hauptman matrices. Acta Crystallogr. A**46** (1990) 688–692.

de Gelder, R.; de Graaff, R. A. G.; Schenk, H.: Automatic determination of crystal structures using Karle-Hauptman matrices. Acta Crystallogr. A**49** (1993) 287–293.

International Tables for X-Ray Crystallography (Volume C.). D. Reidel, Dordrecht, The Netherlands, 1992.

Jacques, J.; Collet, A.; Wilen, S. H.: Enantiomers, Racemates and Resolutions. Wiley-Interscience, New York, 1981.

Jaworski, C.; Hartung, W. H.: Amino alcohols. XII Optical isomers in the ephedrine series of compounds. J. Org. Chem. **8** (1943) 564–571.

Jeffrey, G. A.; Saenger, W.: Hydrogen Bonding in Biological Structures. Springer-Verlag, Berlin, 1991.

Larsen, S.; deDiego, H. L.; A study of two polymorphic modifications of (S)-1-phenylethylammonium (S)-mandelate and the structural features of diastereomeric mandelate salts. Acta Crystallogr. B**49** (1993) 303–309.

Sheldrick, G.: A program for solution of crystallographic structures from x-ray diffraction data. University of Göttingen, Göttingen, Germany 1993.

Sheldrick, G.: A program for refinement of crystallographic structures from x-ray diffraction data. University of Göttingen, Göttingen, Germany 1997.

Valente, E. J.; Miller, C. W.; Zubkowski, J.; Eggleston, D. S.; Shui, X.: Discrimination in resolving systems II: Ephedrine-substituted mandelic acids. Chirality **7** (1995) 652–676.

Valente, E. J.; Zubkowski, J.; Eggleston, D. S.: Discrimination in resolving systems: Ephedrine-mandelic acid. Chirality **4** (1992) 494–504.

Valente, E. J.; Moore, M. C.; Knight-Williams, P. M.: Discrimination in resolving systems. III: Pseudoephedrine-mandelic acid. Chirality **10** (1998) 325–337.